GA–A23348

SEEING SHELL WALL FLUCTUATIONS

by
R.B. STEPHENS, T. MROCZKOWSKI, AND J. GIBSON

JUNE 2000

DISCLAIMER

This report was prepared as an account of work sponsored by an agency of the United States Government. Neither the United States Government nor any agency thereof, nor any of their employees, makes any warranty, express or implied, or assumes any legal liability or responsibility for the accuracy, completeness, or usefulness of any information, apparatus, product, or process disclosed, or represents that its use would not infringe privately owned rights. Reference herein to any specific commercial product, process, or service by trade name, trademark, manufacturer, or otherwise, does not necessarily constitute or imply its endorsement, recommendation, or favoring by the United States Government or any agency thereof. The views and opinions of authors expressed herein do not necessarily state or reflect those of the United States Government or any agency thereof.

GA–A23348

SEEING SHELL WALL FLUCTUATIONS

by
R.B. STEPHENS, T. MROCZKOWSKI,† AND J. GIBSON

†Copper-Union, New York, New York

This is a preprint of a paper to be presented at the 13th Target Fabrication Meeting, November 8–11, 1999, Catalina Island, California and to be published in *Fusion Technology*.

Work supported by
the U.S. Department of Energy
under Contract No. DE-AC03-95SF20732

GA PROJECT 3748
JUNE 2000

SEEING SHELL WALL FLUCTUATIONS

Richard B. Stephens, Tony Mroczkowski,† and Jane Gibson
General Atomics, P.O. Box 85608, San Diego, California 92186-5608
†Cooper-Union, New York, New York

ABSTRACT

Irregularities in ICF shells need to be characterized in detail. Outside and inside surface, and wall thickness fluctuations are all Raleigh-Taylor unstable and can cause a shell to fail during compression. Until recently we could only detect outside surface profile fluctuations, measured along three mutually perpendicular great circles and displayed as line graphs. Measurements, paths, and display have all been upgraded to improve our ability to see fluctuations. We have added a Wallmapper that can determine thickness along the same paths as the surface profiles. The thickness data can be subtracted from the outer surface profile to give a (low resolution) inner surface profile. We have measured the surface profiles along up to 8 paths, and have displayed these profiles wrapped around the image of a sphere. With sufficient paths, this format gives a sense of the 2-D surface fluctuations on the shell. These additions should help us to understand the nature of shell defects and optimize our production processes.

I. INTRODUCTION

When ICF fuel capsules are compressed by ablation of their outer layers, small fluctuations in the surface properties are Rayleigh-Taylor unstable; small deformations can rapidly grow large enough to destroy the shell integrity, contaminate the compressed fuel, and limit ultimate compression. The growth rate of these fluctuations depends on the size of the fluctuation, with the most serious effects occurring around mode number[a]10 to 30[1] These fluctuations are essentially invisible to normal optical inspection; they have neither sharply defined edges which would show up under a microscope as dark lines, nor sufficient curvature to cause a noticeable lensing effect. To date, shells are evaluated for these fluctuations using an Atomic Force Microscope on a smoothly rotating shell [AFM Spheremapper,[2] (Fig. 1)] to trace the surface profile along three mutually orthogonal great circles. These 1-dimensional profiles are Fourier-transformed to yield power spectra that are averaged and compared to a reference curve of allowed fluctuation intensities. Neither the profiles nor the power spectra give much sense of the sources of the fluctuations, and are not very useful for optimizing the shell production process.

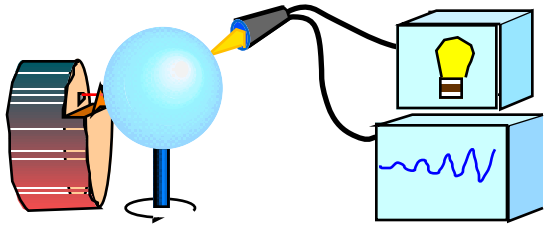

Fig. 1. Sketch of a shell mounted on a rotating vacuum chuck. On the left is the Spheremapper's atomic force microscope head. On the right is the Wallmapper's optical fiber, connected to a light source to illuminate the shell, and a spectrometer to analyze the reflections.

We have recently enhanced our characterization technique in three ways:

1. A Wallmapper has been added to the Spheremapper so that wall thickness and surface profiles can be taken along identical paths,
2. we have collected up to eight profiles on a single shell, and
3. we have wrapped our profile data around an image of a sphere, so that we can see the relationship between the profiles and get a better sense of the two-dimensional structure of the surface.

The Wallmapper setup and resulting data will be described in the next two sections, followed by examples of combined Spheremapper-Wallmapper profiles and the phenomena we can see in them. Sections IV and V describe an alternative profile set and display, and the insights feasible with that approach.

[a]The mode number is the shell circumference divided by the fluctuation wavelength.

II. OPTICAL WALLMAPPING SETUP

The optical wallmapper is based on a device made by Filmetrics.[3] It uses a fiber optic harness to illuminate a thin film sample and return the reflected light to a spectrometer (Fig. 1). The interference oscillations in the reflected spectrum are used to determine the film thickness. We modified the fiber harness to minimize the illuminated spot and control its location, and wrote software to combine the thickness measurements with shell angle. Our adaptation of this device uses a single 100 µm diameter optical fiber to deliver the light and another to detect the reflection[4] A microlens[5] focuses the light and detected area to a ~100 µm diameter spot.

The lens is mounted on our AFM Spheremapper platform, about 200 degrees away from the AFM head (Fig. 2). As a result, surface profiles, taken with the Spheremapper, and wall thickness traces, taken with the Wallmapper, can be taken along identical paths. A shaft encoder on the rotating vacuum chuck ensures that their coordinate systems are synchronized. By combining pairs of Spheremapper and wallmapper data, we can determine the inner surface profile of a shell.

The Wallmapper is somewhat incompatible with the Spheremapper, so they cannot yet make measurements simultaneously. The most intractable problem is that light from the diode laser in the AFM head scatters into the Wallmapper collection optics. Either the AFM head must be moved back from the shell during Wallmapper measurements, or the Wallmapper must restrict its analysis spectrum to avoid the diode wavelength (790 nm).

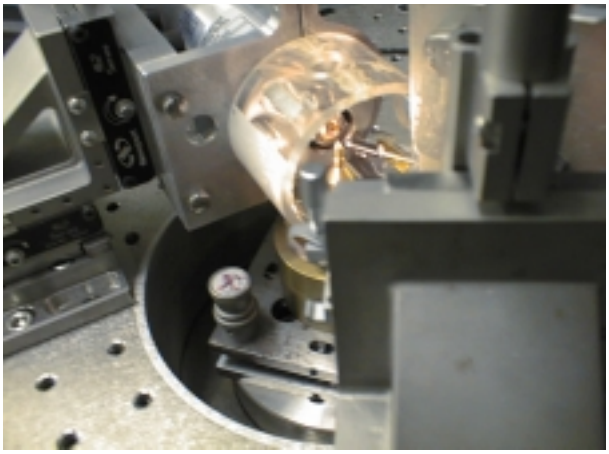

Fig. 2. The Spheremapper table showing the brass rotating vacuum chuck on top of its tilt table. The AFM head is behind the vacuum chuck and holds a plastic windshield around the sample. The Wallmapper optic probe is coming in toward the shell from the front right.

III. OPTICAL WALLMAPPING DATA

We take data points as close together as possible, so that each analysis can take the previous result as a good starting guess. As a result, Wallmapper measurements are made with the shell rotating at the equipment's slowest speed of 1/4 rpm (most Spheremapper measurements are taken at 1 rpm). Since the analysis of each measurement takes usually less than 5 s (mostly analysis time) we can take ~45 measurements per rotation, and collect data over three rotations to obtain adequate data. Occasionally the analysis time takes longer—up to 10 s—to converge on an answer, and the following measurement is delayed. The result is a set of 135 irregularly spaced thickness measurements, each averaging the wall thickness over a ~100 µm diameter spot. In contrast, Spheremapper data sets contain 3600 evenly spaced points with nearly atomic resolution. They record fluctuations from dust particles that are too small to affect the Wallmapper measurements.

These disparate data sets need preparation before they can be combined. Both data sets are smoothed to the Wallmapper resolution (using Gaussian smoothing with a width of 6 degrees — ~100 µm for a 2 mm diameter shell), then interpolated to get new data sets with values at 1 degree intervals, and finally subtracted to give the inner surface profile. Before the profiles are plotted, the average value (mode 0) is removed from all the profiles, and the rotation axis offset (mode 1) from the surface curves. Figures 3(a) and 3(b) show data sets for two different kinds of shells for three mutually orthogonal paths on each shell.

IV. COMBINED WALLMAPPER/ SPHEREMAPPER DATA

Figure 3(a) shows a data set (outside surface, wall thickness, and inside surface for three paths, and average power spectra for the surfaces and wall) from a bare Poly(α-Methyl Styrene) (PAMS) mandrel. The variation in wall thickness shows a non-concentricity between the inside and outside surfaces; the wall has no shorter wavelength fluctuations. The structure seen in the outer surface profile is caused by folding of a nearly uniformly thick wall, rather than denting of the outside surface.

Figure 3(b) shows a data set from a Glow Discharge Polymer (GDP) shell made on a PAMS mandrel, like the one shown in Fig. 3(a). A 3 µm thick GDP shell was deposited on the PAMS, and the PAMS removed. Then a Poly(Vinyl Alcohol) (PVA) gas barrier layer (averaging 3 µm thick) was added, followed by 20 µm more of

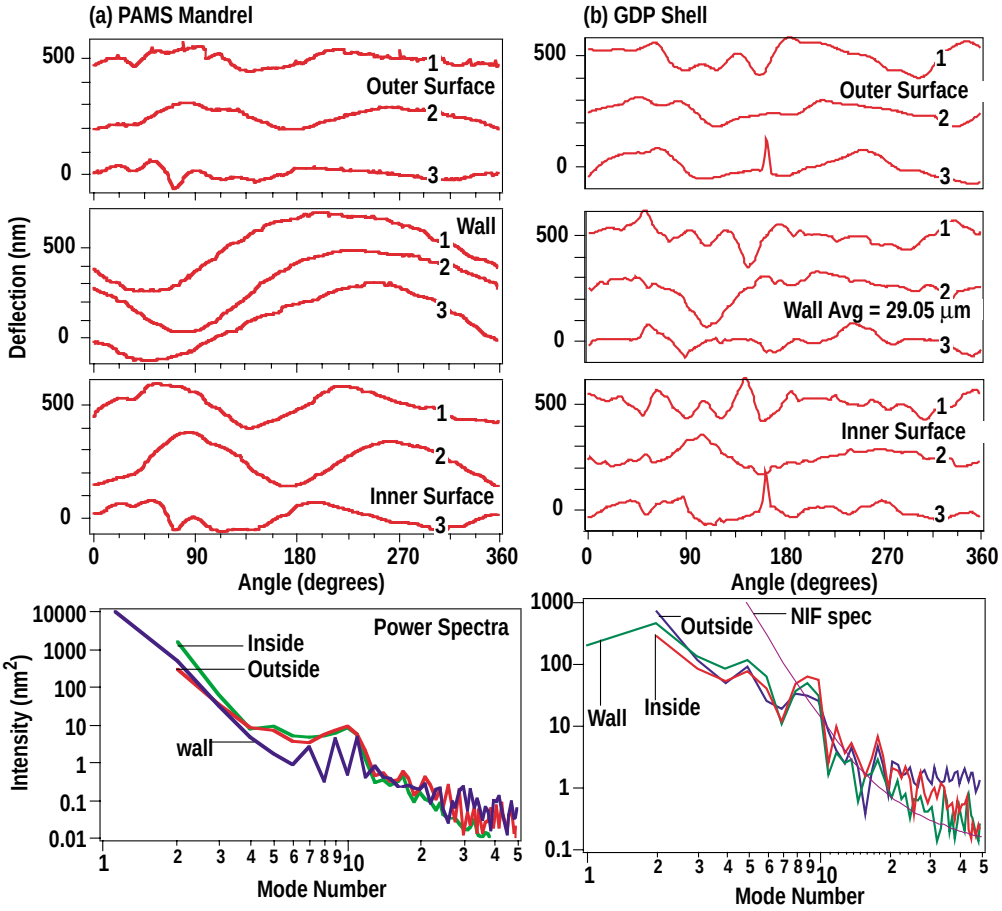

Fig. 3. Outside surface, wall thickness, inside surface, and power spectra along three paths for (a) a bare PAMS mandrel, and (b) a GDP/PVA/GDP shell made from such a mandrel.

GDP. The profiles for this shell differ markedly from those of the bare PAMS. The outer surface shows considerably larger short wavelength oscillations. As expected, these oscillations are nearly duplicated in the wall thickness; it is well known that PVA tends to form a lumpy layer. But we did not expect to find the calculated inner surface also to be lumpy. We expected the GDP inner surface [Fig. 3(b)] to be similar to the PAMS outer surface [Fig. 3(a)] since the GDP shell was formed on a PAMS mandrel. It is possible that the lumpy PVA, when it shrank, strained the shell enough to fold the inside a bit. It is also possible that the subtraction technique is not sufficiently accurate to cancel large fluctuations. We do not have an independent tool to check these possibilities.

V. SPHERICAL REPRESENTATION OF SURFACE PROFILES

Although surface profiles show fluctuations, and power spectra of those profiles give a quantitative representation of their amplitude, neither is of much use in process development. For that purpose we need to understand the forces that generate the fluctuations, and for that we need to be able to visualize the 2-D surface they represent. Our normal set of three mutually orthogonal 1-D traces is no help in 2-D visualization [Fig. 4(b)]. Adding more traces is not much help either [Fi. 5(b)].

We found that Igor Pro[6] contains a surface plotter routine which allows us to wrap those 1-D profiles

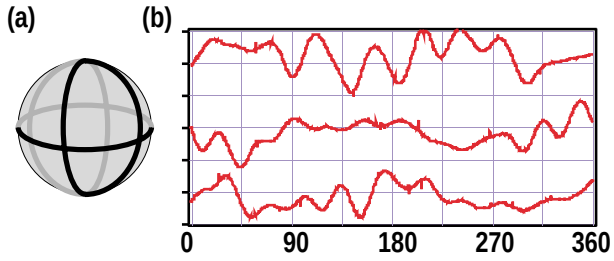

Fig. 4. (a) Standard paths used for spheremapping and (b) Typical profiles along those paths.

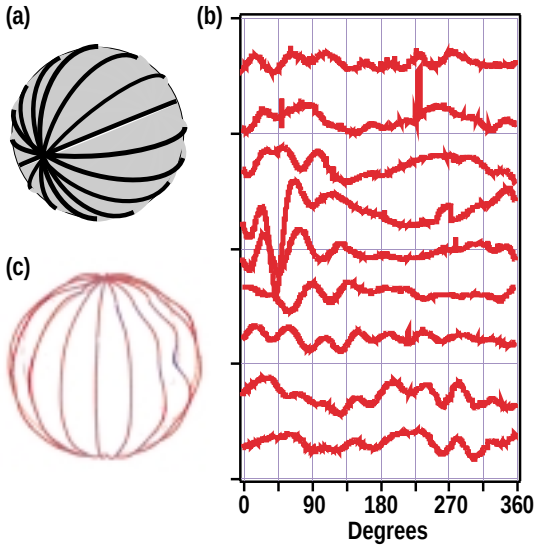

Fig. 5. (a) Paths rotating 22.5° around a single axis, (b) the profiles along those paths, and (c) the same profiles wrapped around a sphere.

around the image of a sphere. That format allows a much better understanding of the 2-D nature of the surface [Fig. 5(c)].

Even the biggest of the fluctuations we deal with are tiny compared to the radius of the shell, so we generally magnify the fluctuations by 300-500 times. Igor Pro also provides the capability to rotate the shell on the screen, and even to set it spinning freely. Motion helps considerably in interpreting the surface.

VI. TYPICAL SURFACE FLUCTUATIONS

Figure 6(b) shows typical surfaces for shells with large fluctuations. The surfaces look like they have wrinkled as a result of a local impact rather than shrinking (like a prune).

Figure 6(a) shows some shells that are much smoother; they exhibit a small elongation along one axis. This is the kind of effect one expects from stirring-induced shear while the shell was curing.

VII. SUMMARY

We have improved our shell characterization capability by combining a Wallmapper with a Spheremapper, changing the measured path pattern, and developing a 2-D surface display. These modifications allow us to get new information, or to see it from a new point of view, thereby helping shell process development. The new data show, for instance, how stresses from uneven PVA layers could be wrinkling the shells, and how stirring of the curing baths could be stretching them

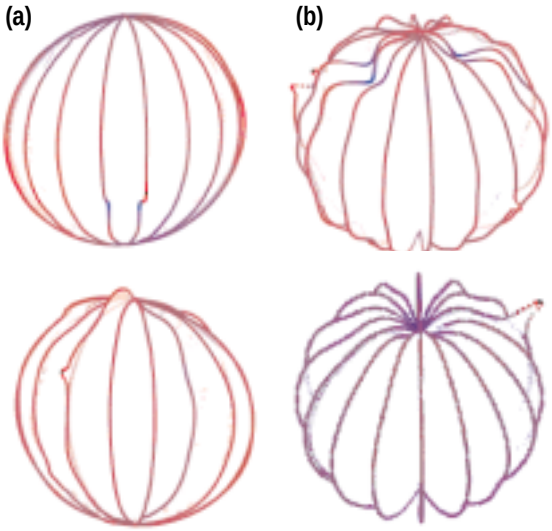

Fig. 6. Sphere-wrapped profiles showing (a) shear-induced distortion and (b) localized dents and surface debris. The profiles have been magnified 300X relative to the shell size.

out. They also show patterns of surface wrinkling which we do not yet understand; whether dents are caused by propeller impacts or some other cause, they cannot be eliminated unless they can be seen.

IV. ACKNOWLEDGMENTS

Work supported by the U.S. Department of Energy under Contract No. DE-AC03-95SF20732.

REFERENCES

1. J. Lindl, “Development of the indirect-drive approach to inertial confinement fusion and the target physics basis for ignition and gain,” *Phys. Plasmas* **2** 3933-4021 (1995).
2. The GA Spheremapper is essentially a duplicate of the original developed at LLNL described by R.L. McEachern, C.E. Moore, and R.J. Wallace, “Description, performance, and application of an atomic force microscope based profilometer,” *J. Vac. Sci. & Techn.* **A 13** #3 983 (1995).
3. Filmetrics, 7675 Dagget St, Suite 140, San Diego, CA 92111.
4. This is a bifurcated fiber optic bundle, with each arm containing one 100 µm diameter fiber. The fibers are encased in a 1 mm diameter s.s. hypodermic tube for the last few inches at the shell end, and separated only by their cladding at the end. As a result, light source and spectroscopic detector are both focussed on the same spot.
5. We used a SELFOC® Microlens (NSG America, Western Regional Office, 950 South Coast Drive, #260, Costa Mesa, CA 92626) as a relay lens whose end faces are 1.9 mm focus distance from the fibers, and 1.1 mm from the shell.
6. Igor Pro version 3.0 by Wavemetrics, Inc., P.O. Box 2088, Lake Oswego, Oregon 97035.